Adaptive Passivity-based Hybrid Pose/Force Control for Uncertain Robots

Antonio C. Leite*, Francisco L. Cruz*, Fernando Lizarralde**

* *Norwegian University of Life Sciences,*
Faculty of Science and Technology, Ås, Norway
(e-mail: antonile@nmbu.no).
** *COPPE-Federal University of Rio de Janeiro,*
Department of Electrical Engineering, Rio de Janeiro RJ, Brazil
(e-mail: fernando@coep.ufrj.br).

Abstract: In this work, we consider a novel adaptive hybrid pose/force control strategy for uncertain robot manipulators capable of performing interaction tasks on poorly structured environments. A unique hybrid control law, based on an orientation-dependent term, is proposed to overcome the performance degradation of the feedback system due to the presence of uncertainties in the geometric parameters of the contact surfaces. A gradient-based adaptive law, which depends on the tracking error, is designed to deal with parametric uncertainties in the robot kinematics and the stiffness of the environment. In our solution, the effect of the uncertain robot dynamics is addressed by using an adaptive dynamic control based on a cascade control strategy. The Lyapunov stability theory and the passivity paradigm are employed to carry out the stability analysis of the overall closed-loop control system. Numerical simulations are included to illustrate the performance and feasibility of the proposed methodology.

Keywords: Nonlinear adaptive control, robots manipulators, uncertain dynamic systems, Lyapunov stability, passivity-based control, cascade control.

1. INTRODUCTION

In the last four decades, researchers from robotics community have developed advanced control strategies to combine force/torque and position/velocity measurements in order to allow robots to successfully perform a variety of interaction and manipulation (I&M) tasks. Typical examples include industrial applications (e.g., polishing, contour following), or simple case studies (e.g., sliding on a planar surface, turning a crank), which are described by artificial and natural constraints of force and motion (Villani and De Schutter, 2016). In this context, the well-known hybrid control strategy combines force/moment data with position/orientation information, according to the concept of complementary orthogonal subspaces in force and motion introduced by Mason (Mason, 1981) and experimentally verified on a Scheinman-Stanford arm.

Robotic systems such as dual-arm robots, parallel robots, and multi-fingered robot hands have to face different challenges such as parametric uncertainties in their kinematic and dynamic models, compliant and rigid environments and external disturbances (Madani and Moallem, 2011; Ren et al., 2017). Indeed, commercial grippers and end-effectors, commonly used to carry out interaction tasks with poorly structured environments, have to manipulate specialized tools with different sizes and shapes in the presence of friction forces and uncertain stiffness (Heck et al., 2016; Kanakis et al., 2018). Following this trend, a number of force/motion control algorithms, based on adaptive and robust techniques or even on a combination of both, have been developed enabling uncertainty and disturbance compensation (Pliego-Jiménez and Arteaga-Pérez, 2015; Solanes et al., 2018). Recently, artificial intelligence-based algorithms have also been designed to cope with the aforementioned issues but, in most of them, the lack of a rigorous stability analysis of the overall closed-loop system is still an open and challenging problem (Peng et al., 2019; Rani and Kumar, 2019). Robot control architectures that unify the interaction and motion controllers have been developed by using a suitable combination of vision and force sensing (Leite et al., 2009; Cheah et al., 2010), and the presence of uncertainties in the system parameters have also been of concern. However, in the majority of these publications the *orientation control problem* were not rigorously taken into account in the control design, particularly when the robot motion is constrained on rigid surfaces with *nonplanar* geometry and *uncertain* stiffness.

This manuscript is a follow-up of our previous works (Leite et al., 2009, 2010), where the robot kinematics and the environment stiffness were assumed to be *fully known*. In this work, we address the adaptive hybrid pose/force control problem for robot manipulators with uncertain kinematics capable of performing interaction tasks on contact surfaces with regular curvature. A novel hybrid control law, based on an orientation-dependent term, is proposed to solve the interaction problem on rigid surfaces with uncertain geometric parameters. To deal with the existence of parametric uncertainties in the robot kinematics and environment stiffness, we use an indirect adaptive kinematic control. The uncertain robot dynamics

---

⋆ Independent Researcher, 60115 Street 208A/1363, El Roble, Puntarenas, Costa Rica, (e-mail: franciscolostalo@gmail.com).

is also considered in the proposed solution by using a direct adaptive dynamic control and a cascade control strategy. The stability analysis of the overall closed-loop system is developed based on the Lyapunov stability theory and the passivity paradigm. Numerical simulations, with a 6-DoF robot manipulator interacting on a cylindrical contact surface, illustrate the performance and feasibility of the proposed methodology.

2. ROBOT KINEMATICS

In this section, we consider the kinematic model of an n-DoF robot manipulator in contact with the environment. Let $p \in \mathbb{R}^3$ be the end-effector position with respect to the robot base, expressed in the base frame $\mathcal{F}_b$ and $R_{be} \in \mathbb{SO}(3)$ be the rotation matrix of the tool frame $\mathcal{F}_e$ with respect to the base frame $\mathcal{F}_b$. Now, let $q = [\,q_s\;\; q_v^\mathsf{T}\,]^\mathsf{T}$ be the *unit quaternion* representation for R_{be}, where $q_s \in \mathbb{R}$ and $q_v \in \mathbb{R}^3$ are the scalar and vector parts of the quaternion respectively, subject to the unit norm constraint $q^\mathsf{T} q = 1$. In this context, the end-effector pose $\mathbf{x} \in \mathbb{R}^m$ can be given by the *forward kinematics* map and denoted by a vector function as:

$$\mathbf{x} = \begin{bmatrix} p \\ q \end{bmatrix} = \begin{bmatrix} h(\theta) \\ g(\theta) \end{bmatrix}, \qquad (1)$$

where $\theta \in \mathbb{R}^n$ is the vector of manipulator joint angles. In general, $h(\cdot) : \mathbb{R}^n \mapsto \mathbb{R}^3$ and is a nonlinear mapping between the joint space $\mathcal{Q}$ and the operational space $\mathcal{O}$ and $g(\cdot) : \mathbb{R}^n \mapsto \mathbb{R}^4$ is a nonlinear function which depends on the elements of rotation matrix (Siciliano et al., 2010). The end-effector velocity $\mathbf{v} = [\,\dot{p}\;\; \omega\,]^\mathsf{T}$, composed of the linear velocity $\dot{p} \in \mathbb{R}^3$ and the angular velocity $\omega \in \mathbb{R}^3$, both expressed in the tool frame $\mathcal{F}_e$, is related to the joint velocity $\dot{\theta} \in \mathbb{R}^n$ by the *differential kinematics* equation as:

$$\mathbf{v} = J(\theta)\,\dot{\theta} = \begin{bmatrix} J_p(\theta) \\ J_o(\theta) \end{bmatrix} \dot{\theta}, \qquad (2)$$

where $J(\theta) \in \mathbb{R}^{6 \times n}$ is the manipulator geometric Jacobian matrix, $J_p(\theta) \in \mathbb{R}^{3 \times n}$ and $J_o(\theta) \in \mathbb{R}^{3 \times n}$ are the position and orientation Jacobian matrices respectively. Notice that, the position Jacobian matrix $J_p(\theta)$ can be computed analytically as $J_p(\theta) = (\partial h(\theta)/\partial \theta)$, whereas the orientation Jacobian matrix $J_o(\theta)$ can be computed analytically as $J_o(\theta) = J_r(q)\,(\partial g(\theta)/\partial \theta)$, where $J_r(q)$ is the representation Jacobian matrix, such as $\omega = J_r(q)\,\dot{q}$. It is worth mentioning that the kinematics models (1) and (2) have the following properties very useful for the subsequent control design and stability analysis of any robot manipulator with revolute joints (Siciliano et al., 2010):

Property 1. The Jacobian matrix $J(\theta)$ is bounded for all possible values of θ, that is, $\|J(\theta)\|_\infty \leq c_0$ for $\forall \theta \in [0, 2\pi]$ where $c_0 \in \mathbb{R}^+$ is a positive constant.

Property 2. The forward kinematics mapping (1) can be linearly parameterized by:

$$h(\theta, a_k) = Y_h(\theta)\,a_k, \qquad (3)$$

and the product between the Jacobian matrix $J(\cdot)$ and any measurable vector $\nu \in \mathbb{R}^n$ can be linearly parameterized by:

$$J(\theta, a_k)\,\nu = Y_j(\theta, \nu)\,a_k, \qquad (4)$$

where $Y_h(\theta) \in \mathbb{R}^{3 \times n_k}$ is the *forward kinematics regressor* matrix, $Y_j(\theta, \nu) \in \mathbb{R}^{6 \times n_k}$ is the *differential kinematics regressor* matrix, $a_k \in \mathbb{R}^{n_k}$ is the vector of constant kinematic parameters, assumed to be bounded, and $n_k \in \mathbb{N}$ is the number of kinematic parameters.

2.1 Kinematic Control

Now, considering the *kinematic control* approach, the robot motion can be simply described by:

$$\dot{\theta}_i = u_i, \quad i = 1, \cdots, n, \qquad (5)$$

where $\dot{\theta}_i$ are the angular velocity of the i-th joint and u_i is the velocity control signal applied to the i-th joint motor drive. This assumption can be applied to most commercial robots with high gear reduction ratios and/or when the robot motions are performed with low velocities and slow accelerations. In such cases, the effects of nonlinear coupling terms of the robot dynamics can be neglected and the kinematic control approach ensures a satisfactory performance for the feedback system (Siciliano et al., 2010). Thus, replacing (5) into (2), we obtain the following control system:

$$\mathbf{v} = J(\theta)\,u. \qquad (6)$$

A Cartesian control signal $v_k(t)$ can be transformed into joint control signals $u \in \mathbb{R}^n$ by using a simple *inverse kinematics* algorithm:

$$u = J^\dagger(\theta)\,v_k, \qquad v_k = \begin{bmatrix} v_p^\mathsf{T} & v_o^\mathsf{T} \end{bmatrix}^\mathsf{T}, \qquad (7)$$

where $J^\dagger = J^\mathsf{T}(JJ^\mathsf{T})^{-1}$ is the right pseudo-inverse matrix of $J(\theta)$, which is assumed to be *full row* rank. Therefore, substituting (7) into (6), we have:

$$\mathbf{v} = v_k \qquad \Rightarrow \qquad \begin{bmatrix} \dot{p} \\ \omega \end{bmatrix} = \begin{bmatrix} v_p \\ v_o \end{bmatrix}, \qquad (8)$$

and naturally $v_p \in \mathbb{R}^3$ and $v_o \in \mathbb{R}^3$ are designed to control the position and orientation of the robot end-effector respectively. Notice that, the relationship (8) is valid if, and only if, the following two assumptions hold: (A1) the robot kinematics is *known* exactly; (A2) the control law $v_k(t)$ does not drive the robot manipulator to *singular configurations*. The failure of any of these assumptions is a key issue in robotics, and has been widely investigated in recent years (Leite and Lizarralde, 2016).

2.2 Pose Control

First, consider the position control problem for an n-DoF robot manipulator. We assume that the objective of the control design is to find a suitable control law $v_p(t)$ which ensures that the current end-effector position p tracks a desired position trajectory $p_d(t)$. The *control goal* is simply described by: (i) $p \to p_d(t)$; (ii) $e_p = p_d(t) - p \to 0$, where $e_p \in \mathbb{R}^3$ is the position tracking error. Thus, by using a feedforward plus proportional control law

$$v_p = \dot{p}_d + K_p\,e_p, \qquad K_p = K_p^\mathsf{T} > 0, \qquad (9)$$

where $\dot{p}_d \in \mathbb{R}^3$ is the desired linear velocity and $K_p \in \mathbb{R}^{3 \times 3}$ is the position gain matrix, the position error dynamics is governed by $\dot{e}_p + K_p\,e_p = 0$ which implies that $\lim_{t \to \infty} e_p(t) = 0$. ∎

Now, consider the orientation control problem for an n-DoF robot manipulator. We assume that the objective of the control design is to find a suitable control law $v_o(t)$ which ensures that the current end-effector orientation R tracks a desired orientation trajectory $R_d(t)$. The *control goal* is simply described by: (i) $R \to R_d(t)$; (ii) $R_q = R^\mathsf{T} R_d(t) \to I$, where $R_q \in \mathbb{SO}(3)$ is the orientation error matrix expressed in the tool frame $\mathcal{F}_e$. Notice that, taking $R_d(t) = (R_{be})_d$ and $R = R_{be}$ yields $R_q = R_{be}^\mathsf{T}\,(R_{be})_d$.

Let $e_q = [\, e_{qs} \;\; e_{qv}^\mathsf{T} \,]^\mathsf{T}$ be the unit quaternion representation for R_q such that $e_q = q^{-1} \otimes q_d(t)$, where q and $q_d(t)$ are the unit quaternion representation for R and $R_d(t)$ respectively, and $\otimes$ denotes the quaternion product operator. Notice that, $e_q = [\, 1 \;\; 0^\mathsf{T} \,]^\mathsf{T}$ if and only if R and R_d are aligned. Thus, by using a feedforward plus proportional control law

$$v_o = \omega_d + K_o\, e_{qv}\,, \qquad K_o = K_o^\mathsf{T} > 0\,, \qquad (10)$$

where $\omega_d \in \mathbb{R}^3$ is the desired angular velocity and $K_o \in \mathbb{R}^{3\times 3}$ is the orientation gain matrix, the equilibrium point $(e_{qs}, e_{qv}) = (\pm 1, 0)$ is *almost globally* asymptotically stable. For a proof, please see (Leite et al., 2009). ∎

3. ADAPTIVE KINEMATIC CONTROL

From the robotics literature, it is well-known that the kinematic and dynamic parameters of the robot arm are modified when its end-effector is manipulating different objects with uncertain dimensions. Other sources of uncertainties also arise, for example, when the robot arm is using an automatic tool changer (ATC) system, which provides more versatility to carry out a number of service tasks and flexibility to handle higher payloads. Thus, it is clear that the existence of uncertainties in the robot kinematics and dynamics is a relevant issue, which may be addressed separately as two independent problems. In this context, to deal with the performance degradation and other undesirable effects caused by uncertain robot kinematic and dynamic models, it is imperative to employ adaptive or robust control strategies (Slotine and Li, 1991).

Remark 1. In this work, we assume that: (A3) the inaccuracy in the robot modeling is only due to the existence of uncertainties in its physical and geometric parameters. Therefore, uncertainties related to measurement errors due to offsets of the joint transducers will not be taken into account. This means that kinematic uncertainties only affect position and linear velocity coordinates.

Firstly, let us consider that the forward kinematics map is *uncertain.* In such a case, from *Property 2*, the position of the robot end-effector can be estimated by:

$$\hat{p} = \hat{h}(\theta, \hat{a}_k) = Y_h(\theta)\, \hat{a}_k\,, \qquad (11)$$

where $\hat{a}_k \in \mathbb{R}^{n_k}$ is the estimated kinematic parameter vector. Let $\epsilon \in \mathbb{R}^3$ be the prediction error obtained from the difference between the estimated and the measured positions of the robot end-effector, that is

$$\epsilon = p - \hat{p} = p - Y_h(\theta)\, \hat{a}_k = Y_h(\theta)\, \tilde{a}_k\,, \qquad (12)$$

where $\tilde{a}_k := a_k - \hat{a}_k$ is the parametric error. Notice that, both p and $Y_h(\theta)$ are required to be measured from the system signals. Then, the only uncertain variable in (12) is the kinematic parameter vector $\hat{a}_k$. Thus, a gradient-based adaptive law for updating $\hat{a}_k$ is given by:

$$\dot{\hat{a}}_k = \Gamma_h\, Y_h^\mathsf{T}(\theta)\, \epsilon\,, \qquad \Gamma_h = \Gamma_h^\mathsf{T} > 0\,, \qquad (13)$$

where $\Gamma_h \in \mathbb{R}^{3\times n_k}$ is the adaptation gain matrix, which implies that all system signals are bounded and $\lim_{t\to\infty} \epsilon(t) = 0$. For a proof, please see (Leite and Lizarralde, 2016). ∎

Now, let us consider that the position Jacobian matrix $J_p(\theta)$, computed analytically, is also *uncertain*. In such a case, from *Property 2*, the linear velocity of the robot end-effector can be estimated as:

$$\dot{\hat{p}} = \hat{J}_p(\theta, \hat{a}_k)\, \dot{\theta} = Y_p(\theta, \dot{\theta})\, \hat{a}_k\,, \qquad (14)$$

where $Y_p(\theta) \in \mathbb{R}^{3\times n_k}$ is the position part of the *forward kinematics regressor* matrix, and, considering only the position control problem, the inverse kinematics algorithm (7) takes the form:

$$u = \hat{J}_p^\dagger(\theta)\, v_p\,. \qquad (15)$$

Notice that, the *direct adaptive control* method can not be applied to solve the adaptive control problem since we can not ensure that (15) is linearly parameterized. In this case, it is necessary to resort to the *indirect adaptive control* method, which consists of estimating the uncertain kinematic parameter and then using such an estimate to update the Jacobian matrix and compute the control law.

From *Property 2*, the differential kinematics equation can be written as:

$$\dot{p} = \hat{J}_p(\theta)\, u + Y_p(\theta, \dot{\theta})\, \tilde{a}_k\,. \qquad (16)$$

Then, substituting (15) into (16) and using (9), we can show that the position error dynamics is governed by

$$\dot{e}_p + K_p\, e_p = -Y_p(\theta, \dot{\theta})\, \tilde{a}_k\,. \qquad (17)$$

The uncertain kinematic parameter $\hat{a}_k$ can also be adjusted by using a gradient-based adaptive law as:

$$\dot{\hat{a}}_k = -\Gamma_p\, Y_p^\mathsf{T}(\theta, \dot{\theta})\, e_p\,, \qquad \Gamma_p = \Gamma_p^\mathsf{T} > 0\,, \qquad (18)$$

where $\Gamma_p \in \mathbb{R}^{3\times n_k}$ is the adaptation gain matrix, which implies that all system signals are bounded and $\lim_{t\to\infty} e_p(t) = 0$. For a proof, please see (Leite and Lizarralde, 2016). ∎

4. HYBRID POSITION/FORCE CONTROL

In this section, we consider the motion and interaction control problem for an n-DoF robot manipulator in contact with poorly structured environments by using the *hybrid control approach* (Villani and De Schutter, 2016). The key idea behind this approach is that different directions of the operational space $\mathcal{O}$ are simultaneously controlled by using position and force measurements, according to the concept of *complementary orthogonal subspaces* (Mason, 1981). Thus, the position and force constraints can be specified independently and the designed controllers are not affected by mutual interference. In general, such constraints are defined in a coordinate system which is suitable for task execution, the so-called *constraint frame* $\mathcal{F}_s$ (Siciliano et al., 2010). From appropriate *selection matrices* $S_p \in \mathbb{R}^{3\times 3}$ and $S_f \in \mathbb{R}^{3\times 3}$, which define what degrees of freedom must be controlled by position and force, the control signals can be decoupled. Hence, the control laws for each subspace can be separately designed in order to achieve simultaneously different position and force requirements for a given motion and interaction task. Thus, the *classical* hybrid control law can be given by:

$$v_h = v_{h_p} + v_{h_f}\,, \qquad (19)$$

where $v_{h_p} \in \mathbb{R}^3$ and $v_{h_f} \in \mathbb{R}^3$ are the decoupled control signals acting respectively in the position and force subspaces, such that:

$$v_{h_p} = R_{es}\, S_p\, R_{es}^T\, v_p\,, \qquad v_{h_f} = R_{es}\, S_f\, R_{es}^T\, v_f\,, \qquad (20)$$

where v_p is the position control signal, v_f is the force control signal and R_{es} is the rotation matrix of the constraint frame $\mathcal{F}_s$ with respect to the tool frame $\mathcal{F}_e$. Notice that, from (20) the decoupling of control variables can be carried out in the constraint space $\mathcal{C}$, where the task

is naturally prescribed and the selection matrices, S_p and S_f, have a diagonal form with *null* and *unitary* elements.

A methodology to estimate the geometric parameters of the contact surface in the presence of the friction force and to reorient the robot end-effector on the contact surface can be found in (Leite et al., 2009, 2010).

4.1 Force Control

Consider the force control problem for an n-DoF robot manipulator equipped with a force/torque sensor. We assume that the objective of the control design is to find a suitable control law $v_f(t)$ which ensures that the current end-effector force f tracks a desired force trajectory $f_d(t)$ on a constraint surface. The control goal is simply described by: (i) $f \to f_d(t)$; (ii) $e_f = f - f_d(t) \to 0$, where $e_f \in \mathbb{R}^3$ is the force tracking error. Similarly to *Hooke's law*, the interaction force between the robot end-effector and the environment can be given by the elastic model:

$$f_e = K_s (p - p_s), \qquad (21)$$

where p is the end-effector position at the contact point, $K_s = k_s I$ is the stiffness matrix, $k_s > 0$ is the stiffness coefficient, assumed to be *fully known*, and p_s is the rest position of the environment. Notice that, the vector of contact force f_e has the opposite direction to the vector of end-effector force f, that is, $f_e = -f$. From (8) and considering $v_p = v_f$, implies that $\dot{p} = v_f$. Thus, by using a feedforward plus proportional control law

$$v_f = K_s^{-1} (K_f e_f - \dot{f}_d), \qquad K_f = K_f^\mathsf{T} > 0, \qquad (22)$$

where $\dot{f}_d \in \mathbb{R}^3$ is the time-derivative of the desired force trajectory and $K_f \in \mathbb{R}^{3 \times 3}$ is the force gain matrix, the force error dynamics is governed by $\dot{e}_f + K_f e_f = 0$ which implies that $\lim_{t \to \infty} e_f(t) = 0$. ∎

Remark 2. Here, without loss of generality, we assume that the interaction force between the robot end-effector and the environment occurs by means of a *linear spring* mounted to the force sensor plate, aligned with the end-effector approach axis. In such a case, the stiffness coefficient k_s of the constraint surface can be represented by the *spring constant*, which is the measure of the spring's stiffness (Leite et al., 2009; Siciliano et al., 2010).

Then, based on the well-known Model Reference Adaptive Control (MRAC) approach (Slotine and Li, 1991), a reference model for the desired force trajectory $f_d(t)$ can be obtained by:

$$\dot{f}_m = -\Lambda f_m + \Lambda f_d(t), \qquad \Lambda = \Lambda^\mathsf{T} > 0, \qquad (23)$$

where $f_m \in \mathbb{R}^3$ is the reference model output and $\Lambda \in \mathbb{R}^{3 \times 3}$ is a gain matrix. From the force model (21) and the reference model (23), an *ideal* force control law v_f^* can be given by:

$$v_f^* = k_s^{-1} \Lambda (f - f_d). \qquad (24)$$

Defining the force tracking error as $\epsilon_f := f - f_m$, we obtain the following force error dynamics:

$$\dot{\epsilon}_f = -\Lambda \epsilon_f + k_s v_f - \Lambda (f - f_d). \qquad (25)$$

Then, the usual parameterization for the *direct adaptive control* is given by:

$$v_f = \Omega(f) \hat{\phi}, \quad \Omega(f) = \Lambda (f - f_d), \quad \hat{\phi} = \hat{k}_s^{-1}, \qquad (26)$$

which results in

$$\dot{\epsilon}_f = -\Lambda \epsilon_f + k_s \tilde{v}_f, \qquad \tilde{v}_f = v_f^* - v_f = \Omega(f) \tilde{\phi}, \qquad (27)$$

where $\Omega(f) \in \mathbb{R}^3$ is the *force regressor* vector, $\hat{\phi}$ is the estimated compliance parameter, and $\tilde{\phi} := \phi - \hat{\phi}$ is the parametric error. Thus, a gradient-based adaptive law for updating $\hat{\phi}$ is given by:

$$\dot{\hat{\phi}} = -\gamma_f \Omega^\mathsf{T}(f) \epsilon_f, \qquad (28)$$

where $\gamma_f > 0$ is the adaptation gain, which implies that all system signals are bounded and $\lim_{t \to \infty} \epsilon_f(t) = 0$. For a proof, please see (Leite and Lizarralde, 2016). ∎

4.2 Adaptive Hybrid Kinematic Control

Consider the hybrid position-force control problem for an n-DoF robot manipulator in contact with a constraint surface with *uncertain* geometry. In such a case, the orientation of the robot end-effector must be continuously updated during the interaction task. Here, in contrast to our previous work (Leite et al., 2010), we assume that the *robot kinematics* and the *stiffness coefficient* of the constraint surface are also *uncertain*. Then, the adaptive kinematic control, developed in Section II, could be used to deal with the system performance degradation due to the presence of kinematic and stiffness uncertainties. Hence, considering the hybrid position-force and orientation control problem, the inverse kinematics algorithm (7) takes the form:

$$u = \hat{J}^\dagger(\theta) v_k, \quad v_k = \begin{bmatrix} \tilde{v}_h \\ v_o \end{bmatrix}, \quad \hat{J}^\dagger(\theta) = \begin{bmatrix} \hat{J}_p^\dagger(\theta) \\ \hat{J}_o^\dagger(\theta) \end{bmatrix}, \qquad (29)$$

where the *novel* hybrid control law

$$\tilde{v}_h = \tilde{v}_{h_p} + \tilde{v}_{h_f}, \qquad (30)$$

includes a *new term*, that depends on the end-effector orientation, in the decoupled position and force control signals, that is:

$$\tilde{v}_{h_p} = \hat{R}_{es} S_p \hat{R}_{es}^\mathsf{T} v_p + \hat{R}_{es} S_p Q(\omega_{es}) \hat{R}_{es}^\mathsf{T} e_p, \qquad (31)$$

$$\tilde{v}_{h_f} = \hat{R}_{es} S_f \hat{R}_{es}^\mathsf{T} v_f + \hat{R}_{es} S_f Q(\omega_{es}) \hat{R}_{es}^\mathsf{T} \hat{K}_s^{-1} e_f, \qquad (32)$$

where $\omega_{es} \in \mathbb{R}^3$ is the angular velocity of the constraint frame $\mathcal{F}_s$ with respect to the tool frame $\mathcal{F}_e$, assumed to be *measurable* from the system signals, $Q(\cdot)$ is the skew-symmetric operator and $\hat{K}_s = \hat{k}_s I$ is the *uncertain stiffness* matrix. Now, let $\xi_p \in \mathbb{R}^2$ be decoupled position error and $\xi_f \in \mathbb{R}$ be the decoupled force error, both expressed in the constraint frame $\mathcal{F}_s$, after selecting the position and force control directions, such that, $\xi_p^\mathsf{T} \xi_p = \bar{e}_p^\mathsf{T} \bar{e}_p$ with $\bar{e}_p = S_p R_{es}^\mathsf{T} e_p$ and $\xi_f^\mathsf{T} \xi_f = \bar{e}_f^\mathsf{T} \bar{e}_f$ with $\bar{e}_f = S_f R_{es}^\mathsf{T} \epsilon_f$, where $\bar{e}_p \in \mathbb{R}^3$ and $\bar{e}_f \in \mathbb{R}^3$. Then, the following notable theorem can be stated:

Theorem 1. Consider the closed-loop system described by (6) and (29) with the kinematic adaptation law (18), the hybrid control law given by (30) and (31)-(32), the position controller (9), the force controller (26) with the adaptation law (28), and the orientation controller (10). Assume that the reference signal $p_d(t)$, $f_d(t)$ are piecewise continuous and uniformly bounded in norm, and $q_d(t)$ is the unit quaternion representation for $R_d(t) \in SO(3)$. Then, under the assumption (A2), the following properties hold: (i) all signals of the closed-loop system are uniformly bounded; (ii) $\lim_{t \to \infty} \xi_p(t) = 0$, $\lim_{t \to \infty} \xi_f(t) = 0$ and $\lim_{t \to \infty} e_{qv}(t) = 0$, $\lim_{t \to \infty} e_{qs}(t) = \pm 1$. Thus, the overall closed-loop system is *almost globally* asymptotically stable.

The proof follows from (Leite et al., 2010, Theorem 1). ∎

Notice that, the aforementioned theorem allow us to establish passivity properties for the adaptive hybrid kinematic control scheme. Suppose the hybrid control system is driven by a fictitious external input signal $\nu = [\,\nu_p^{\mathsf{T}} \;\; \nu_o^{\mathsf{T}}\,]^{\mathsf{T}}$, the error system can be rewritten as:

$$\dot{e}_p = \dot{p}_d - (v_h + \nu_p)\,, \tag{33}$$

$$\dot{e}_f = -\dot{f}_d - \hat{K}_s\,(v_h + \nu_p)\,, \tag{34}$$

$$\dot{e}_q = J_r^{\mathsf{T}}(e_q)\,(\omega_d - v_o - \nu_o)\,, \tag{35}$$

where $\nu_p = \hat{J}_p(\theta)\,\sigma$ and $\nu_o = J_o(\theta)\,\sigma$. Then, after defining the matrices $\Sigma_p = R_{bs}\,S_p\,R_{bs}^{\mathsf{T}}$ and $\Sigma_f = R_{bs}\,S_f\,R_{bs}^{\mathsf{T}}\,K_s$, we can state the following corollary:

Corollary 1. Consider the error system (33)-(35), the hybrid control law (19) with (31) and (32), and the orientation control law (10). Then, the maps $\mathcal{M}_p : \nu_p \mapsto \hat{R}_{es}(S_p K_p^{-1}\bar{e}_p + S_f K_f^{-1}\bar{e}_f)$ and $\mathcal{M}_o : \nu_o \mapsto e_{qv}$ are *output strictly passive* with positive definite *storage function* $V_h = V_p + V_o$ given by $V_h(\bar{e}_p, \bar{e}_f, \tilde{a}_k, \tilde{\phi}, e_{qs}, e_{qv}) = \bar{e}_p^{\mathsf{T}}\bar{e}_p + \bar{e}_f^{\mathsf{T}}\bar{e}_f + \Gamma_p^{-1}\tilde{a}_k^{\mathsf{T}}\tilde{a}_k + \gamma_f^{-1}|k_s|\tilde{\phi}^2 + 2\,(e_{qs}-1)^2 + 2\,e_{qv}^{\mathsf{T}}\,e_{qv}$.

The proof follows from (Leite et al., 2010, Corollary 1). ∎

5. ROBOT DYNAMICS

Now, we recall that the nonlinear robot dynamics in the absence of friction and other disturbances can be expressed in the joint space $\mathcal{Q}$ in terms of generalized coordinates as (Siciliano et al., 2010):

$$M(\theta)\ddot{\theta} + C(\theta, \dot{\theta})\dot{\theta} + G(\theta) = \tau - J^{\mathsf{T}}(\theta)\,F\,, \tag{36}$$

where $\tau \in \mathbb{R}^n$ is the vector of actuation torques, $F \in \mathbb{R}^6$ the vector of generalized forces, that is, $F = [\,f^{\mathsf{T}} \;\; \mu^{\mathsf{T}}\,]^{\mathsf{T}}$ is the vector of forces $f \in \mathbb{R}^3$ and moments $\mu \in \mathbb{R}^3$ exerted by the robot end-effector on the environment, $M(\theta) \in \mathbb{R}^{n \times n}$ is the manipulator inertia matrix, $C(\theta, \dot{\theta})\,\dot{\theta}$ is the torque vector due to the action of Coriolis and centrifugal forces, and $G(\theta) \in \mathbb{R}^n$ is the torque vector of gravitational forces acting at the joints. Considering the dynamic model of an n-DoF robot manipulator (36), some notable properties very useful for deriving control algorithms can be found in (Siciliano et al., 2010) and some of them are presented in the following:

Property 3. The left-hand side of (36) can be linearly parameterized by the term $Y(\theta, \dot{\theta}, \ddot{\theta})\,a_d$, that is

$$M(\theta)\ddot{\theta} + C(\theta, \dot{\theta})\dot{\theta} + G(\theta) = Y_d(\theta, \dot{\theta}, \ddot{\theta})\,a_d\,, \tag{37}$$

where $Y_d(\theta, \dot{\theta}, \ddot{\theta}) \in \mathbb{R}^{n \times n_d}$ is the *dynamic regressor* matrix, $a_d \in \mathbb{R}^{n_d}$ is the vector of constant dynamic parameters, assumed to be bounded, and $n_d \in \mathbb{N}$ is the number of dynamic parameters.

Property 4. From *Property 2*, the external torques acting at the joints, due to the generalized forces, can be linearly parameterized as

$$J^{\mathsf{T}}(\theta, a_k)\,F = Y_s(\theta, F)\,a_k\,, \tag{38}$$

where $Y_s(\theta, F) \in \mathbb{R}^{n \times n_k}$ is the static regressor matrix. In such a case, we can show that $J_p^{\mathsf{T}}(\theta)\,f = Y_s(\theta, f)\,a_k$, provided that only the position coordinates are affected by kinematic uncertainties.

5.1 Cascade Control Strategy

In this section, the key idea is to introduce a *cascade control strategy* to solve the hybrid position-force control

problem for a robot manipulator with nonnegligible dynamics. Such a control strategy can be designed simply by cascading two passivity-based adaptive controllers, one kinematic and one dynamic, analogous to our earlier works on vision-based robot control (Leite et al., 2009; Leite and Lizarralde, 2016). Then, let us assume that there exist a dynamic control law $\tau = k(\theta, \dot{\theta}, \theta_d, \dot{\theta}_d, \ddot{\theta}_d)$ which ensures the control goal defined by

$$\theta \to \theta_d(t)\,, \qquad e = \theta_d(t) - \theta \to 0\,. \tag{39}$$

where $e \in \mathbb{R}^n$ is the joint position error vector and $\theta_d \in \mathbb{R}^n$ is the desired position trajectory previously planned in the joint space $\mathcal{Q}$ and assumed to be uniformly bounded. Now, suppose we can define θ_d and its time-derivatives $\dot{\theta}_d, \ddot{\theta}_d$ as a function of the Cartesian control signal $v_k(t)$ such that we have (8), except for a *vanishing perturbation* term $w(t)$ in its right-hand side as:

$$\mathbf{v} = v_k + w\,, \qquad w = J(\theta)\,L(s)\,e\,, \tag{40}$$

where $L(\cdot)$ denotes a linear operator, possibly non-causal, and s is the differential operator. Then, we can conclude that the Cartesian controller $v_k(t)$ designed to the kinematic control case can be applied to (40) and the stability properties of the closed-loop control system still holds.

In this context, we can show that the hybrid position-force control scheme based on the kinematic control approach has passivity properties, which allows for ensuring the closed-loop stability when it is connected in cascade with a dynamic control scheme with similar passivity properties. Here, we will use the general result for *passive interconnected control systems* subject to external disturbances, as stated in the (Leite and Lizarralde, 2016, Theorem 1).

5.2 Adaptive Dynamic Control

Now, let us consider the existence of parametric uncertainties in the robot kinematics and dynamics, given by (2) and (36) respectively. In this context, we will show that the control design for the robot manipulator can be derived by simply cascading the proposed hybrid position-force scheme with a *modified* Slotine-Li Adaptive Control scheme (Slotine and Li, 1991). First, we consider the following signals defined in the joint space $\mathcal{Q}$ as:

$$\dot{\theta}_r := \dot{\theta}_d - \Lambda e\,, \qquad \sigma := \dot{\theta} - \dot{\theta}_r = \dot{e} + \Lambda e\,, \tag{41}$$

where $\dot{\theta}_r \in \mathbb{R}^n$ is a velocity reference signal and $\sigma \in \mathbb{R}^n$ is a virtual velocity error and $\Lambda = \Lambda^{\mathsf{T}} > 0$ is a gain matrix.

From *Property 3* and *Property 4*, we assume that the robot dynamic model (36), in the presence of parametric uncertainties can be expressed in terms of the regressor matrices as $\hat{M}(\theta)\,\ddot{\theta}_r + \hat{C}(\theta, \dot{\theta})\dot{\theta}_r + \hat{G}(\theta) = Y_d(\theta, \theta, \dot{\theta}_r, \ddot{\theta}_r)\,\hat{a}_d$ and $\hat{J}^{\mathsf{T}}(\theta)F = Y_s(\theta, F)\,\hat{a}_k$ respectively. A *novel* dynamic control law can be given by:

$$\tau = Y_d(\theta, \theta, \dot{\theta}_r, \ddot{\theta}_r)\,\hat{a}_d - K_d\,\sigma + Y_s(\theta, F)\,\hat{a}_k + u_2\,, \tag{42}$$

where $\hat{a}_d \in \mathbb{R}^{n_d}$ is the estimated dynamic parameter vector, $u_2 \in \mathbb{R}^n$ is a fictitious external input, which drives the closed-loop system and $K_d = K_d^{\mathsf{T}} > 0$ is a gain matrix. The vectors of estimated kinematic and dynamic parameters, $\hat{a}_k$ and $\hat{a}_d$, can be adjusted by using the following gradient-based adaptive laws:

$$\dot{\hat{a}}_k = -\Gamma_k\,(Y_p^{\mathsf{T}}\,e_p + Y_s^{\mathsf{T}}\,\sigma)\,, \qquad \Gamma_k = \Gamma_k^{\mathsf{T}} > 0\,, \tag{43}$$

and

$$\dot{\hat{a}}_d = -\Gamma_d Y_d^{\mathsf{T}} \sigma, \qquad \Gamma_d = \Gamma_d^{\mathsf{T}} > 0, \qquad (44)$$

where Γ_k and Γ_d are the adaptive gain matrices for the kinematic and dynamic parameters respectively. The stability analysis and passivity properties of the closed-loop system can be stated by the following theorem:

Theorem 2. Consider the robot dynamic model (36), the dynamic control law (42) and the adaptation laws (43) and (44). Assume that the regressor matrices Y_d, Y_p and Y_s are measured from the system signals. Then, the map $\mathcal{M}_d : u_2 \mapsto \sigma$ is *output strictly passive* with the definite positive *storage function* V_d given by $2V_d(\sigma, \tilde{a}_k, \tilde{a}_d) = \sigma^{\mathsf{T}} M(\theta)\sigma + \tilde{a}_k^{\mathsf{T}}\Gamma_k^{-1}\tilde{a}_k + \tilde{a}_d^{\mathsf{T}}\Gamma_d^{-1}\tilde{a}_d$ and for $u_2 = 0$, the following properties hold: (i) all signals of the closed-loop systems are uniformly bounded; (ii) $\lim_{t\to\infty} \sigma(t) = 0$, which implies that $\lim_{t\to\infty} \dot{e}(t), e(t) = 0$.

For a proof, please see (Leite and Lizarralde, 2016). ∎

5.3 Cascade Passivity-based Systems

Now, the key idea is to apply the cascade control strategy previously presented in (Leite et al., 2009) to generate the reference signals for the robot dynamic control. Following the cascade framework, we can define:

$$\dot{\theta}_r(t) := \hat{J}^{\dagger}(\theta) v_k, \qquad (45)$$

and by using the forward kinematics mapping (1) and the virtual velocity error (41), the motion of the robot end-effector in the operational space $\mathcal{O}$ is governed by:

$$\mathbf{v} = v_k + \hat{J}(\theta)\sigma + d(\theta, \dot{\theta}), \qquad (46)$$

where $\sigma \in \mathbb{R}^n$ can be considered as a *vanishing disturbance* term, provided that from *Theorem 2* it converges to zero, and $d \in \mathbb{R}^6$ is a *kinematic disturbance* term, which depends on the uncertain robot kinematics. Then, the cascade strategy can be implemented by simply setting

$$\dot{\theta}_m(t) := \hat{J}^{\dagger}(\theta) v_k - \Lambda e. \qquad (47)$$

Now, considering the passivity properties of the adaptive hybrid position-force control (see *Corollary 1*) and the adaptive dynamic control (see *Theorem 2*) we can apply the main result of (Leite and Lizarralde, 2016, Theorem 1) to analyze the overall stability of the interconnected systems. The cascaded subsystems $\mathcal{S}_1$ and $\mathcal{S}_2$ are identified by their corresponding states respectively as

$$x_1 = [\bar{e}_p^{\mathsf{T}} \ \bar{e}_f^{\mathsf{T}} \ \tilde{\phi} \ e_{qv}^{\mathsf{T}}]^{\mathsf{T}}, \qquad x_2 = [e^{\mathsf{T}} \ \dot{e}^{\mathsf{T}} \ \tilde{a}_k^{\mathsf{T}} \ \tilde{a}_d^{\mathsf{T}}]^{\mathsf{T}},$$

and by their corresponding outputs respectively as:

$$y_1 = \hat{J}_p^{\mathsf{T}}(\theta)(\Sigma_p \bar{e}_p + \Sigma_f \bar{e}_f) + J_o^{\mathsf{T}}(\theta) e_{qv}, \qquad y_2 = \sigma,$$

where $d(\theta, \dot{\theta}) = Y_p(\theta, \dot{\theta})\tilde{a}_k$ is a bounded disturbance term. The storage functions $V_1(x_1)$ and $V_2(x_2)$ are defined as

$$V_1(x_1) = V_h(\bar{e}_p, \bar{e}_f, \tilde{\phi}, e_{qs}, e_{qv}), \qquad V_2(x_2) = V_d(\sigma, \tilde{a}_k, \tilde{a}_d).$$

Therefore, by using the main result of (Leite and Lizarralde, 2016, Theorem 1), we can show that (i) all signals of the closed-loop subsystems are uniformly bounded, (ii) $\tilde{a}_k, \tilde{\phi}, \tilde{a}_d \in \mathcal{L}_\infty$, (iii) $\lim_{t\to\infty} \sigma(t) = 0$, and consequently $\lim_{t\to\infty} \dot{e}(t), e(t) = 0$, (iv) $\lim_{t\to\infty} \bar{e}_p(t), \bar{e}_f(t) = 0$, $\lim_{t\to\infty} e_{qv}(t) = 0$, and consequently $\lim_{t\to\infty} e_{qs}(t) = \pm 1$, which demonstrate the *almost global* asymptotic stability of the interconnected closed-loop systems. ∎

6. NUMERICAL SIMULATIONS

In this section, we present simulations results to illustrate the performance of the proposed adaptive kinematic hybrid control scheme. In the simulations, a 6-DoF robot manipulator has to perform the tracking of a reference trajectory on a cylindrical surface with uncertain stiffness and geometry. The robot links lengths are $l_1 = 279.4 \ mm$, $l_2 = 228.6 \ mm$ and $l_3 = 92.3 \ mm$ for links 1, 2 and 3 respectively. The reference trajectory is prescribed in yz plane and given by $p_d(t) = [0 \ r_n \cos(2\omega_n t) \ r_n \sin(\omega_n t)]^{\mathsf{T}} + p(0)$, where $r_n = 100 \ mm$ and $\omega_n = \frac{\pi}{5} \ rad \, s^{-1}$ are the radius and the angular velocity of the trajectory respectively, with $p(0)$ being the initial position of the end-effector given by the forward kinematics map as $p(0) = h(\theta(0))$ with $\theta(0) = [0 \ \frac{\pi}{3} \ \frac{-7\pi}{6} \ \pi \ \frac{-\pi}{3} \ \frac{\pi}{2}]^{\mathsf{T}} \ rad$. The control parameters are: $K_p = 20 \, I \ mm \, s^{-1}$, $K_f = 40 \, I \ mm \, s^{-1} N^{-1}$, $K_o = 10 \, I \ rad \, s^{-1}$, $\Gamma_p = 20 \, I$ and $\gamma_f = 2$. Other parameters are: $f_d = 10 \ N$, $k_s = 10 \ N \, mm^{-1}$ and $\Lambda = 2$. We also consider that the link lengths and the stiffness coefficient have uncertainty levels around 20% and 50%, respectively.
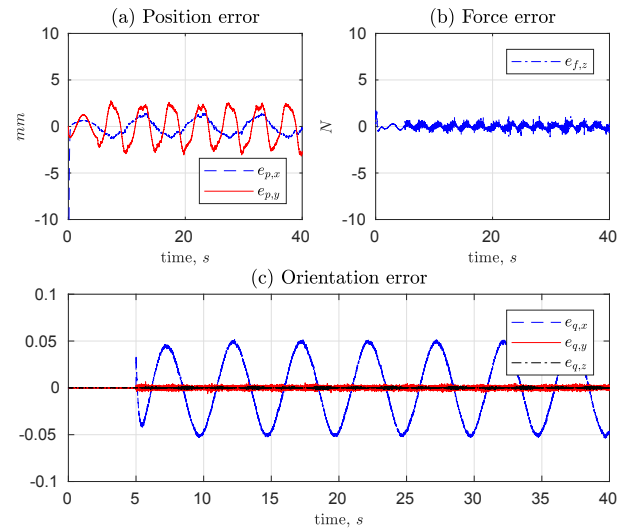

Fig. 1. Position, force and orientation errors.

In the numerical simulations, the end-effector orientation was kept constant until the approaching phase ends, when the contact point on the surface has been reached at $t = 5 \ s$. Figures 1(a) and 1(b) describe the behavior over time of the position and force errors respectively. The maximum peak of position and force errors in the steady-state were around $2.5 \ mm$ and $1.0 \ N$, respectively. The time history of decoupled position and force control signals are presented in Figures 2(a) and 2(b) respectively. Figures 1(c) and 2(c) describe the behavior over time for the orientation error and orientation control signal respectively. The norm of the orientation error in the steady-state was around 2×10^{-2}. The tracking of the reference trajectory, a Lissajous curve, is depicted in Fig. 3(a), where it can be noticed that a remarkable performance was achieved during the motion/interaction task. In Fig. 3(b), it is depicted the trajectory followed by the robot end-effector on an uncertain cylindrical surface located in the workspace. The time history of the parameter estimation is shown in Figures 3(c) and 3(d), where it is possible to observe that a fast parametric convergence has been achieved, less than $t = 5 \ s$.
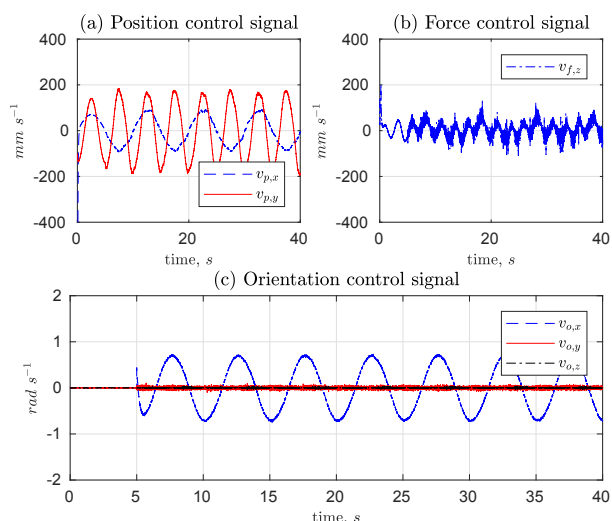
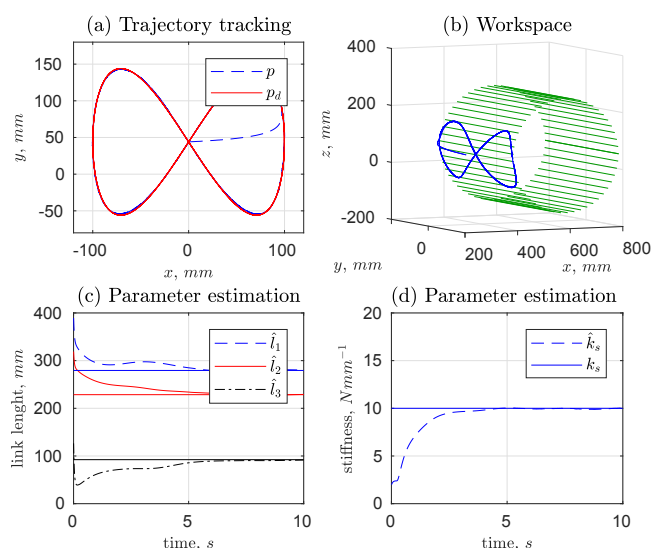Fig. 2. Position, force and orientation control signals.

Fig. 3. Trajectory tracking and parameter estimation.

7. CONCLUDING REMARKS

In this work, we address the adaptive hybrid pose/force control problem for robot manipulators capable of performing motion and interaction tasks on uncertain contact surfaces. A novel adaptive hybrid control strategy, based on an orientation-dependent term, is derived to ensure a satisfactory system performance in the presence of uncertainties in the robot kinematics. A cascade control strategy and an adaptive dynamic control are used to consider the uncertain robot dynamics in our solution. The stability analysis of the overall closed-loop system is developed by using the Lyapunov stability theory and the passivity paradigm. Numerical simulations are included to illustrate the effectiveness and feasibility of the proposed methodology. In future works we intend to carry out experimental tests with robot manipulators performing interaction tasks on uncertain environments, and to extend the adaptive hybrid pose/force control scheme for cooperative robots in object manipulation tasks.

REFERENCES

Cheah, C.C., Hou, S.P., Zhao, Y., and Slotine, J.J.E. (2010). Adaptive Vision and Force Tracking Control for Robots With Constraint Uncertainty. *IEEE/ASME Transactions on Mechatronics*, 15(3), 389–399.

Heck, D., Saccon, A., van de Wouw, N., and Nijmeijer, H. (2016). Guaranteeing Stable Tracking of Hybrid Position-force Trajectories for a Robot Manipulator interacting with a Stiff Environment. *Automatica*, 63, 235–247.

Kanakis, G.S., Dimeas, F., Rovithakis, G.A., and Doulgeri, Z. (2018). Prescribed Contact Establishment of a Robot with a Planar Surface under Position and Stiffness Uncertainties. *Robotics and Autonomous Systems*, 104, 99–108.

Leite, A.C. and Lizarralde, F. (2016). Passivity-based Adaptive 3D Visual Servoing without Depth and Image Velocity Measurements for Uncertain Robot Manipulators. *International Journal of Adaptive Control and Signal Processing*, 30(8-10), 1269–1297.

Leite, A.C., Lizarralde, F., and Hsu, L. (2009). Hybrid Adaptive Vision-Force Control for Robot Manipulators interacting with Unknown Surfaces. *The International Journal of Robotics Research*, 28(7), 911–926.

Leite, A.C., Lizarralde, F., and Hsu, L. (2010). A Cascaded-based Hybrid Position-force Control for Robot Manipulators with Nonnegligible Dynamics. In *Proceedings of the 2010 American Control Conference*, 5260–5265. Baltimore (MD), USA.

Madani, M. and Moallem, M. (2011). Hybrid Position/force Control of a Flexible Parallel Manipulator. *Journal of the Franklin Institute*, 348(6), 999–1012.

Mason, M.T. (1981). Compliance and Force Control for Computer Controlled Manipulators. *IEEE Transactions on Systems, Man, and Cybernetics*, 11(6), 418–432.

Peng, J., Ding, S., Yang, Z., and Zhang, F. (2019). Neural Network-Based Hybrid Position/Force Tracking Control for Robotic Systems Without Velocity Measurement. *Neural Processing Letters*, 51, 1125–1144.

Pliego-Jiménez, J. and Arteaga-Pérez, M.A. (2015). Adaptive Position/force Control for Robot Manipulators in Contact with a Rigid Surface with Uncertain Parameters. *European Journal of Control*, 22, 1–12.

Rani, K. and Kumar, N. (2019). Intelligent Controller for Hybrid Force and Position Control of Robot Manipulators using RBF Neural Network. *International Journal of Dynamics and Control*, 7(2), 767–775.

Ren, Y., Chen, Z., Liu, Y., Gu, Y., Jin, M., and Liu, H. (2017). Adaptive Hybrid Position/force Control of Dual-arm Cooperative Manipulators with Uncertain Dynamics and Closed-chain Kinematics. *Journal of the Franklin Institute*, 354(17), 7767–7793.

Siciliano, B., Sciavicco, L., Villani, L., and Oriolo, G. (2010). *Robotics: Modelling, Planning and Control*. Springer-Verlag London Ltd.

Slotine, J.J.E. and Li, W. (1991). *Applied Nonlinear Control*. Prentice Hall, Inc.

Solanes, J.E., Gracia, L., Muñoz-Benavent, P., Valls Miro, J., Perez-Vidal, C., and Tornero, J. (2018). Robust Hybrid Position-Force Control for Robotic Surface Polishing. *Journal of Manufacturing Science and Engineering*, 141(1), 1–14.

Villani, L. and De Schutter, J. (2016). Force Control. In B. Siciliano and O. Khatib (eds.), *Springer Handbook of Robotics*, 195–220. Springer International Publishing.